Photodissociation of H_2^+ and D_2^+: Experiment*

Friedrich von Busch† and Gordon H. Dunn‡
Joint Institute for Laboratory Astrophysics, §
University of Colorado, Boulder, Colorado 80302
(Received 28 June 1971)

Measurements are reported of the cross sections for photodissociation of H_2^+ and D_2^+ at 21 wavelengths ranging from 2472 to 13 613 Å. The measurements are compared with theory using normalized Franck-Condon factors for the vibrational populations of the ions. Deviations are found, which are interpreted as a failure of this latter approximation. A least-squares analysis of the data yields vibrational-state populations different from simple Franck-Condon factors and alleged to be those characteristic of high-energy electron-impact ionization of H_2 and D_2. Interpretation of the data using a mechanism requiring that a fraction of the ions formed by electron impact be generated via the autoionization channel can qualitatively lead to the observations of this experiment. However, such an explanation would require about $\frac{2}{3}$ of all H_2^+ and D_2^+ to be formed via autoionization—a seemingly unrealistic requirement. Interpretation of the data in terms of a variation with internuclear separation of the electronic matrix element involved in the electron-impact ionization process shows that a matrix element varying as $Q_e(r) = 1 + 0.56(r_{a.u.} - 0.99)^2$ can lead to the experimentally deduced populations of both H_2^+ and D_2^+. This latter interpretation is favored, though one cannot rule out the former or some combination of the two. The data and interpretation are consistent with other related experiments.

I. INTRODUCTION

The H_2^+ ion, being the simplest molecule, has long drawn the attention of theoreticians. The fact that many of its properties and possible reactions can be treated exactly within the usual approximation of separable nuclear and electronic motions, thus allowing sound predictions to compare with experiment, makes it equally interesting from the experimental point of view. It certainly constitutes an excellent point of departure for developing and experimentally testing our concepts and understanding of many molecular processes.

Interest in the H_2^+ ion was boosted further by attempts to achieve thermal fusion of hydrogen in the laboratory and by the advancement of astrophysics. In fact, photodissociation of H_2^+ was first treated theoretically considering astrophysical applications by Bates[1] and by Buckingham *et al.*,[2] whereas the first experimental observation of the process, done in 1957 by Linlor, Barnett, and Reinhardt,[3] was motivated by the hope that it could be successfully employed in the generation of high-temperature hydrogen plasmas. These latter authors passed light from a mercury arc through a beam of H_2^+ ions and obtained the order of magnitude of the average cross section. An approximate calculation pertaining to the above experiment, which dealt with a sample of H_2^+ ions populating all vibrational states, was done by Gibson.[4] In 1963 Dunn reported the first measurement of the cross section in a crossed beam experiment with monochromatic light.[5] Dunn found striking disagreement with Gibson's theoretical predictions. This led him to perform calculations of the process[6] that are nearly exact in the approximation of stationary nuclei. The discrepancy with experiment remained essentially as it was, but it could no longer be blamed on theory. A carefully redesigned experimental investigation appeared desirable, and is the basis of the present work.

Theory[6] gives cross sections σ_v for photodissociation from single vibrational levels v of H_2^+, whereas experiment deals with a mixture of ions in all levels. The experimental situation can be made such that the populations of levels may be expected to be determined by the Franck-Condon factors connecting the ion to the ground state of H_2. In view of the accuracy of the σ_v, this assumption would be the major approximation in a theoretical prediction tailored to the experiment. It therefore would be an experimental goal to test the model and to obtain actual population factors for the vibrational levels. Such an experiment is reported in this paper.

Section II gives an outline of the physics of the process under consideration. A thorough description and discussion of the experimental setup and procedures, including the search for possible systematic errors, constitutes Sec. III. The data obtained are presented and assessed in Sec. IV. Section V contains the discussion and interpretation of the results. Finally, in Sec. VI we investigate the relationship of our results to other experiments.

II. THEORETICAL CONSIDERATIONS

Owing to the simplicity of the H_2^+ system, it has

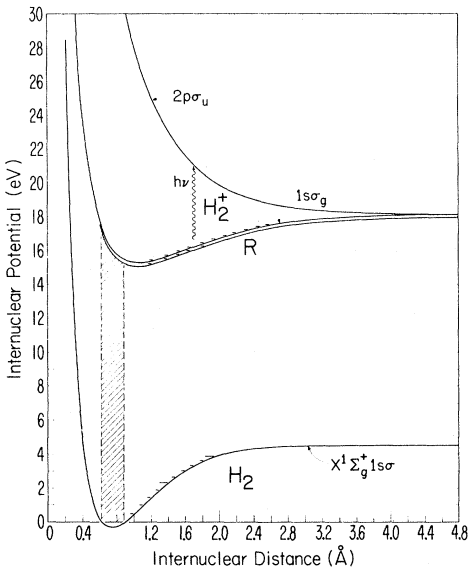

FIG. 1. Internuclear potential curves for H_2 and H_2^+ relevant to this experiment. The curves for H_2^+ are from Ref. 7, and the curve for the $X\,^1\Sigma_g^+$ state of H_2 is from Ref. 25. The Rydberg state R is sketched in as a displaced $1s\sigma_g$ H_2^+ curve. The wavy arrow indicates the transition for which the cross section is measured in this paper.

been possible to do most calculations relevant to photodissociation in an exact way within the usual approximation of separable nuclear and electronic motions (Born-Oppenheimer approximation). Accurate energies for various electronic states[7] as well as oscillator strengths[8] for the pertinent transition have been published. Vibrational eigenenergies have been calculated[9–11] for the electronic ground state of both H_2^+ and D_2^+. Franck-Condon factors for the ionizing transitions from the ground states of H_2 and D_2 to all vibrational levels in the lowest electronic state of the respective molecular ions have also been calculated by a number of workers,[10–12] with the most complete and accurate calculations being those of Villarejo.[11] Of the several calculations[1,2,4,6,13] of the cross section for photodissociation the work of Dunn[6] is the most relevant to use for a comparison with experiment.

Figure 1 gives some of the potential curves for H_2 and H_2^+. An electric dipole interaction of ions in the $1s\sigma_g$ state with light causes transitions to the vibrationally continuous $2p\sigma_u$ state. The molecule dissociates into a ground-state H atom and a proton:

$$H_2^+(1s\sigma_g) + h\nu \rightarrow H_2^+(2p\sigma_u) \rightarrow H(1s) + H^+ . \qquad (1)$$

The outgoing particles share equally the excess energy of the photon over the binding energy of the initial state.

Formation of the H_2^+ target by ionization of H_2 is possible by various means. It is technically possible to generate the molecular ion in controlled vibrational and rotational quantum states by photoionization[14–17] of H_2. Unfortunately, however, number densities of H_2^+ achievable by this method are far too low to allow a subsequent photodissociation experiment. Similar considerations preclude the use of highly monoenergetic electrons to form the H_2^+ target. One is thus led to use ionization of H_2 by bombardment with electrons having an energy large compared to ionization threshold.

The differences in shape and positions of the minima of the potential curves of H_2 and H_2^+ lead, in this case, to the formation of ions with finite populations in all vibrational levels. Radiative lifetimes[18] between the levels are of the order of 10^7 sec, so apart from collisional relaxation the population distribution stays the same throughout the experiment as in the formation process. To carry the theory to a point where it can be compared with experiment, a knowledge of this population distribution is necessary. Then we have for the predicted cross section $\sigma(\lambda)$ at wavelength λ,

$$\sigma(\lambda) = \sum_{v,K} p_{vK}\,\sigma_{vK}(\lambda) , \qquad (2)$$

where p_{vK} is the fractional population of level vK, and $\sigma_{vK}(\lambda)$ is the theoretical[6] photodissociation cross section at λ from vibration-rotation level vK.

The p_{vK} as well as the σ_{vK} depend only weakly on K, so that we can write Eq. (2) as

$$\sigma(\lambda) = \textstyle\sum_v p_v\,\sigma_{v\mathfrak{K}}(\lambda), \qquad (3)$$

where we have assumed (see the Appendix) an effective rotational quantum number $\mathfrak{K}$, $\sigma_{vK}(\lambda) \approx \sigma_{v\mathfrak{K}}(\lambda)$, and $\sum_K p_{vK} = p_v$. In this work we take $\mathfrak{K} = 1$ for H_2^+ and $\mathfrak{K} = 2$ for D_2^+.

No measurements of the p_v have as yet been published. Their computation requires knowledge of the electronic matrix element of the ionizing transition and, as this has not yet been calculated, we make the common assumption that it varies slowly with internuclear separation and thus with vibrational quantum number over the range of distances involved. To a first approximation we may neglect this variation,[19] so that transitions then take place "vertically" from the ground state of H_2, i.e., within the shaded area of Fig. 1. If, furthermore, the energy of the ionizing electrons is large compared to the ionization energies for the various vibrational H_2^+ states, the populations of these states should depend only on the overlap integrals between the initial and final vibrational wave functions involved in the ionizing transition, i.e., they should be determined by normalized Franck-Condon factors. Franck-Condon factors have been used in arriving at the predicted cross sections $\sigma(\lambda)$ re-

ported in the literature.[4,6,13]

Assuming that the photodissociation of H_2^+ can be treated adequately in the Born-Oppenheimer approximation, the theoretical $\sigma_{v\mathfrak{K}}(\lambda)$ are essentially exact, and any discrepancy between the experimental cross section and the calculated composite cross section should then reflect a deviation of the p_v from the Franck-Condon factors. One can expect to get a suitable fit of theory to experiment by taking properly adjusted p_v's in Eq. (3). Any disagreement between the p_v's thus deduced and normalized Franck-Condon factors may probably be ascribed to: (a) inadequacy of the assumption of an electronic transition matrix element that varies slowly with r, and/or (b) strong autoionization of Rydberg states of H_2 in forming H_2^+. These matters will be pursued further in discussing the data.

III. EXPERIMENT

The experiment was performed by crossing a beam of H_2^+ ions with a monochromatic light beam of variable wavelength and the dissociative interaction (1) was detected via the resulting protons. The cross section $\sigma(\lambda)$ is obtained from a formula analogous to that used for the electron impact work[20]:

$$\sigma(\lambda)=\frac{i_{H^+}}{i_{H_2^+}}\frac{v_i}{\phi_\lambda}\frac{}{\Omega}. \tag{4}$$

Here i_{H^+} and $i_{H_2^+}$ are the currents of signal protons and parent molecular ions, respectively, ϕ_λ is the flux of photons of wavelength λ, v_i is the velocity of the molecular ions, and

$$\Omega=[\int R(z)G(z)dz/\int R(z)dz\int G(z)dz]\,C \tag{5}$$

is the beam-overlap factor. $R(z)$ and $G(z)$ are one-dimensional intensity distributions of the ion and light beam, respectively, taken along a coordinate perpendicular to the plane defined by the intersecting beams. The factor C with a value 1.027 is needed because the photon beam is divergent at about 17° half angle, and to first order simply involves the $1/\cos\theta$ path-length correction of the light through the ion beam. Higher-order terms which correct for the inclination between partial rays and the scanning coordinate are found to be entirely negligible.

A major portion of the experiment involved verifying the functional relationships of quantities in Eq. (4) and searching for other hidden parameters the measured cross section might depend upon. Absolute cross sections were measured at wavelengths ranging from 2472 to 13 613 Å.

The experiment is, in many respects, similar to the measurement by Dunn and Van Zyl[20] of the H_2^+ electron-impact dissociation performed with the same ion beam apparatus. We shall therefore touch on points of close resemblance only briefly and refer to the pertinent paper for further details.

A. General Arrangement

The general scheme of the experiment is illustrated in Fig. 2. The H_2^+ ions are formed by electron bombardment of H_2 gas at low pressure, accelerated, and made into a mass-analyzed parallel beam. An intense light beam from a high-pressure arc is passed through a fast grating monochromator and focused onto the intersecting ion beam. Protons generated by the interaction have less than 2.5 eV energy in the c.m. system, compared to typically 8 keV of the molecular ion targets. They therefore leave the interaction region with almost the same speed and direction as the parent ions, carrying half of their energy in the laboratory frame. The two ionic species are separated in a 45° parallel-plate electrostatic analyzer ($\Delta E/E\approx 20\%$) and collected in Faraday cups. The proton current from photodissociation is several orders of magnitude smaller than a proton background arising from breakup collisions of H_2^+ ions with residual gas. Therefore, the light beam is chopped in a symmetric square wave pattern at frequencies of 25–45 Hz. The same is then true of the proton beam originating from photodissociation and, by subsequent phase-sensitive detection, the dc background is rejected.

The light intensity is measured calorimetrically and monitored continuously with a thermopile. The spatial overlap of the crossed beams can be probed by driving two perpendicular slits, one of which carries a photocell behind it, through the region of intersection. Thus, all parameters necessary to measure absolute cross sections according to Eq. (4) can be determined.

The ion beam passes several differentially pumped regions before entering the final interaction chamber. The first of these chambers, next to the ion source, contains some ion optics and is pumped by a 700-liter/sec oil-diffusion pump to typically 2×10^{-7} Torr with 2×10^{-3} Torr H_2 in the source.

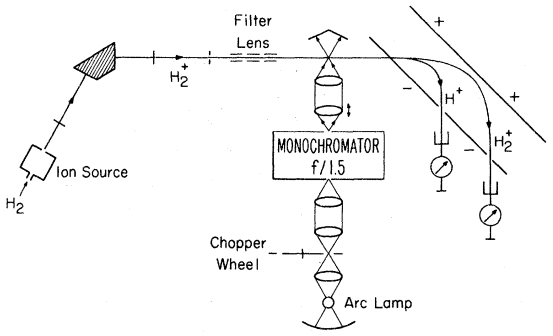

FIG. 2. Schematic representation of the experimental arrangement.

The beam then passes through a magnetic 60° sector mass spectrometer into a second chamber, which also contains focusing elements and is pumped by a 100-liter/sec ion pump to about 2×10^{-8} Torr. From there the beam enters the final chamber, where the interaction takes place. This region is pumped by a 100-liter/sec ion pump. An additional titanium sublimation pump allows faster initial pumpdown. The base pressure attained without bakeout is 2×10^{-10} Torr, and the pressure rises to 10^{-9} Torr when the ion beam is on. Because of the background signal arising from collisions with residual gas, ultrahigh vacuum in the interaction vessel is absolutely necessary.

B. Ion Source and Optics

It is clear from what has been said in Sec. II that the measured cross section crucially depends on the distribution of vibrational quantum states in the irradiated sample of molecular ions. These ions therefore should be generated under conditions which make the distribution depend on as few parameters as possible, thereby optimizing chances of a theoretical prediction (no measurements on this exist yet), and under conditions which do not cause this distribution to change in an uninterpretable way once the ions have been formed. Since the radiative lifetimes of the vibrational states are extremely long,[18] the latter restriction amounts to the exclusion of collisions. The pressure in the ion source therefore has to be so low that collisions can be shown not to affect the measured cross section.

The first condition implies that the ions are formed by electrons with an energy which is high compared to the differences in threshold energies of the various vibrational states. The ratios of the ionization cross sections into these various levels can then be expected to be independent of electron energy. Furthermore, temperature in the source should be low enough so that parent H_2 molecules are in the ground vibrational state, thereby minimizing the range of internuclear distances. These circumstances best justify the application of the Franck-Condon principle in calculating the population distribution of the H_2^+ ions.

The ion source should thus be of the electron bombardment rather than of the discharge type. A slightly modified Bayard-Alpert gauge was used, which has been described earlier.[20] This source typically yielded a 3–4 μA beam of H_2^+ operating at 2-mTorr H_2 pressure and 50 mA of electrons. Beam currents were stable to within a few percent and were reproducible from day to day. The glass envelope of the source had a temperature between 65 and 135 °C, depending upon proximity to a cooling fan. In the analysis in Sec. V, it is assumed that the rotational temperature of the H_2 gas is 100 °C.

Ions were extracted along the axis of the cylindrical grid. The grid was held at + 200 V relative to the filament, and the extracting electrode at − 270 V. A retarding analysis performed on ions in the final beam showed that under these conditions the ions were formed by electrons with energies between 106 and 141 eV, the mean energy being 128 eV. Since the thresholds for forming H_2^+ in various vibrational levels vary between 15.4 and 18 eV, the first condition noted above is satisfied. An alternate potential configuration in the ion source bracketed electron energies to lie between 100 and 300 eV. No retarding analysis was made, but it is likely that the mean energy was around 200 eV. Data taken over a range of wavelengths with this arrangment agreed to within statistical limits with those obtained under the normal operating conditions described above, further verifying that the first condition on the source is met.

A small permanent magnet was attached to the glass envelope of the source opposite the filament. This increased the attainable ion beam by 40–50%. By measurements taken at three different wavelengths, it was demonstrated that the photodissociation cross section did not depend on whether or not the magnet was attached to the source.

Impurities in the source are thought to play a negligible role in the beam formation and its character. A typical mass spectrum shows H^+ [2], H_2^+[94], H_3^+[1], O^+[0.2], OH^+[0.5], H_2O^+[1.3], and N_2^+[0.2] to be present. Here the bracketed numbers show the relative peak heights. There are, of course, other ions present, but with far smaller relative intensities.

The source grid is floated at 8333 V, resulting in a final beam energy of 8261 eV. The ion optical arrangement is the same as described earlier.[20] After passing through the mass spectrometer the beam is made parallel. Before entering the interaction region it passes through a three-element rectangular cylinder lens, which focuses the ions at the center and makes the beam parallel again. The center element is held at such a positive voltage that particles with half the beam energy cannot pass through the lens. The beam thus is cleared of protons formed by breakup collisions with residual gas, which would greatly deteriorate the signal-to-noise ratio. Even the background protons generated downstream from the filter lens in ultrahigh vacuum give a current of about 10^{-12} A compared with a typical photodissociation signal of 5×10^{-15} A.

C. Interaction Region and Analyzer

After passing through the rejection lens the ion beam enters the reaction region. The parallel light beam passes through a quartz window into the vacuum chamber, is focused by a lens onto the point

of interaction with the ion beam, and is then absorbed by a trap coated with platinum black. At the crossing point, the light beam is approximately 5 mm wide and 7 mm high; the ion beam is 1.5 mm wide and typically 5 mm high.

The continuing ions enter the electrostatic energy analyzer, as do the protons formed in the reaction. The analyzer is of the 45° parallel-plate type first built by Yarnold and Bolton[21] and has been described elsewhere.[20] The ions are collected in Faraday cups with a metal honeycomb structure. Electrodes and a bias voltage are suitably arranged to prevent secondary electrons from escaping.

The internal energy of the dissociating H_2^+ ions is converted into kinetic energy of the fragments, thereby causing some angular spread of the signal proton beam. The width of the Faraday cup imposes a limit to the divergence one can tolerate. It has been shown in connection with the electron-impact dissociation experiment by Dunn and Van Zyl[20] that 100% collection efficiency is achieved at 10-keV beam energy for protons having up to 10-eV kinetic energy in the c.m. frame. Since in the present experiment the dissociating proton energy cannot exceed half the energy transformed in the interaction, which at maximum amounts to about 2.5 eV for 2500-Å photons, full collection is assured down to much lower beam acceleration voltages than the 8333 V used throughout.

D. Beam Scanner

Absolute cross-section measurements with intersecting beams require a knowledge of their spatial overlap. In the limit of a "thin" target, the beam profiles have to be scanned at the interaction point in a direction perpendicular to the plane defined by the crossed beams. For the ions this is done by driving a 0.005-in.-wide slit through the beam, so that only the small portion of beam falling within the slit opening can continue its way into the Faraday cup. This slit is located about 1 in. from the interaction region, which is sufficient for the parallel ion beam. The light profile is probed similarly by driving through the light beam a 0.005-in.-wide slit, located in the vertical plane containing the ion beam axis and parallel to that axis. Behind this slit a photocell is mounted, whose chopped signal is detected by phase-sensitive amplification. Both slits are arranged in the same plane on a sled, which is moved vertically into and through the beams by a stepping motor, thus allowing a point scan of both beam profiles at the same time. Since the light probe would intercept half of the ion beam, during a scan the latter is moved parallel to its slit away from the light probe to pass it uninhibited. It was demonstrated that this does not change the profile. The shifting of the beam is accomplished by applying a voltage across the last element of the rejection lens, which is cut in half along the beam axis, thus forming parallel-plate deflectors. Profiles were scanned by driving the slits in steps of 0.005 in. across the beams, taking readings at each step.

E. Light Source

A dc-operated high-pressure short arc serves as a light source. The lamp is mounted in a closed housing and cooled by a stream of forced air. Two lamps, preferentially emitting different parts of the spectrum, have been used. A Hg-Xe lamp with 5-kW rated input power emitting strong Hg lines in the ultraviolet and visible superimposed on a weak continuum was used between 2500 and 5800 Å. In the red and infrared a pure Xe lamp with 2.5-kW rated input was used, which gave quite a strong continuum from 4600 to 10 500 Å, as well as intense lines in the near infrared.

The arc is imaged by $f/1.2$ optics onto the exit slit of the lamp housing, where the light can be intercepted by a shutter. The beam then passes a slotted wheel, which chops it symmetrically at low audio frequency (usually 28 Hz). The light is made parallel and enters a fast grating monochromator ($f/1.2$) of the Ebert type. As the light converges to the fixed exit focus of this instrument, it is angle stopped to a 34° cone angle, and an aperture is located at the focus 7 mm high and 5 mm wide. Made approximately parallel again by a lens, the beam then passes through a window into the vacuum vessel and is focused by another lens into the interaction region. The former of these lenses is moveable to allow imaging of the collimator onto the beam crossover for all wavelengths. The entire optical setup, employing quartz elements and mirrors throughout, provides a 1:1 image of the arc at the beam intersection with a cone angle of 34°. The light, after passing through the interaction region, is collected on a cone covered with platinum black. Reflected light passing through the beam is thus of negligible consequence.

A quartz-plate beam splitter is mounted inside the monochromator at 45° inclination relative to the exit beam, and reflects some 10% of the light through a lens onto a thermopile. The latter serves as a monitor of the relative light intensity.

Two gratings blazed at 4000 and 8000 Å, respectively, were used in the experiment. Colored-glass filters to suppress higher diffraction orders and stray light could be inserted into the beam path at the main and monitor exits of the monochromator. A triangular 200-Å full width at half-maximum bandpass of the instrument was used throughout the experiment. This spectral window $T(\lambda - \lambda^\circ)$ was folded numerically with the output spectrum $F(\lambda)$ taken at 30-Å bandwidth around every nominal wavelength used in taking data, thus yielding actual av-

erage wavelengths $\bar{\lambda}$:

$$\bar{\lambda} = \int T(\lambda - \lambda^\circ)F(\lambda)\lambda d\lambda / \int T(\lambda - \lambda^\circ)F(\lambda)d\lambda \ .$$

Similarly, the quantity $\langle\sigma(\lambda)\rangle$ was computed where

$$\langle\sigma(\lambda)\rangle = \int T(\lambda - \lambda^\circ)F(\lambda)\sigma(\lambda)\lambda\, d\lambda / \int T(\lambda - \lambda^\circ)F(\lambda)\lambda\, d\lambda \ .$$

Integrations were over the range of λ for nonzero $T(\lambda - \lambda^\circ)$.

Here $\sigma(\lambda)$ was taken as the theoretical cross section using Franck-Condon factors for the population factors p_v in Eq. (3). It was shown that at wavelengths used in this experiment, $\sigma(\bar{\lambda}) = \langle\sigma(\lambda)\rangle$ to within 0.4% in every case and to within 0.1% in most cases. The average wavelength $\bar{\lambda}$ is thus used in the discussion and analysis to follow.

Light intensities transmitted in the 200-Å bandpass were typically 40 mW in the visible Xe continuum and 100–200 mW in the strongest Hg lines. The light output is constant within 2% over periods of several hours.

F. Radiometry

Radiometry was done using a power calorimeter, which could be attached to the collimator at the monochromator exit after the light gun had been backed from the ion beam machine. Intensities thus obtained were corrected for the measured transmission of the optical elements between the collimator and the interaction region.

Basically, the calorimeter consists of a receiver cup connected by a rod to a metal block serving as a heat sink. Light absorbed in the cup causes a temperature gradient along the rod, which is proportional to the power input. The basic structure of the calorimeter is made of OFHC copper and is gold plated to reduce radiative losses. The interior of the cup is coated with platinum black. A measurement using 6328-Å light from a He-Ne laser showed that less than 0.15% of the light entering the cup is reflected. The temperature gradient along the rod is measured with thermocouples, whose output is amplified and displayed versus time on a recorder. A heater coil wound around the receiver cup is used to calibrate the device by feeding a known amount of power into it. A sensitivity of 585 ± 3 μV/W of input power and a time constant of about 30 sec was measured. The calorimeter exhibits a small nonlinearity, which could be demonstrated to be caused by air convection. A correction, linear with input power and about 1% per 200 mW, has been applied to the data to account for this convective effect. The sensitivity quoted above is that obtained by extrapolation to zero input power.

Alternatively, the sensitivity may be obtained less accurately by calculation from the geometry of the design and materials constants. Including minor corrections for heat lost by air conduction and radiation we obtain 608 μV/W. This figure, which differs only by about 4% from the measured value, is considered to agree well with the latter when allowance is made for uncertainties in the materials constants and geometric approximations in the calculation.

Drift of the calorimeter zero of 0.2–0.5 μV over periods of several minutes was quite common. Measurements therefore were always made by establishing the zero before and after a reading and interpolating between these values. Readings of the calorimeter thus are accurate to 1% or better.

As already mentioned, part of the light passing through the collimator and measured by the calorimeter does not reach the interaction region, but gets lost by reflection and absorption in the final optical elements, i.e., two lenses and a window. The optical transmission of these elements has been measured for every wavelength used in the experiment. To this end the vacuum vessel was opened and the calorimeter placed in the interaction region. Light intensities measured behind the collimator and at the beam crossover, respectively, were then compared using the monitor to correct for changes in lamp output that occurred while moving the calorimeter from one position to the other. A plot of these transmission data versus wavelength gives a smooth curve, varying from 74% in the infrared to 80% in the visible and to 42% at 2537 Å. It was discovered after the fact of the cross-section measurements that the apparent transmission of these elements was slightly sensitive to various optical adjustments only coarsely recorded during the experiment. This thus gives rise to one of the major systematic uncertainties in the measurements—varying from 2 to 5% depending on wavelength.

G. Data Accumulation

Signal currents are typically on the order of 5×10^{-15} A. Detection of such low currents by ac amplification is limited by noise generated in the input resistor and first amplifier stage, rather than shot noise. This is true even though the modulated signal current is measured against a dc background of about 10^{-12} A originating from dissociative collisions of primary ions on residual gas. Signal-to-noise ratios of about 2 integrating over 1 sec are found. Precise measurements thus require considerable integration times. Though use of a multiplier would have improved the situation, it was precluded by calibration considerations.

The signal proton and H_2^+ currents, together with the output of the light monitor, are integrated by operational amplifiers over periods of 50 sec. A data run consists of 50–80 such integrations taken alternately with the ion beam on and off. This reduces statistical fluctuations in the averaged signal

to typically 2%. Each data run is preceded by calibration of all three data channels and a measurement of the beam overlap factor Ω (cf. Sec. III D). Calibration of the proton channel is done by measuring a beam of N^{++} or O^{++} ions (from impurities in the ion source) in a conventional way, chopping it and feeding it into the collector cup, whereas the dc amplifiers in the H_2^+ channel are calibrated by usual means. The light monitor is calibrated against the calorimeter. The latter is then removed and the light gun is brought up to the ion beam machine for the data run. All data are converted to digital form and recorded on punched paper tape.

Linearity, temperature dependence, and time variation of all relevant electronic devices were studied, and necessary corrections were applied to the data.

H. Systematic Effects

The nature of the experiment makes it susceptible to quite subtle errors. Thus a careful search for spurious signals and other error sources is absolutely necessary. Part of this can be done by varying the parameters contained in Eq. (4) and verifying the proper functional dependences of the signal. Spurious signals giving rise to additive terms in (4) should therefore show up.

Figure 3 demonstrates the proportionality of the signal to the ion and light fluxes, respectively.

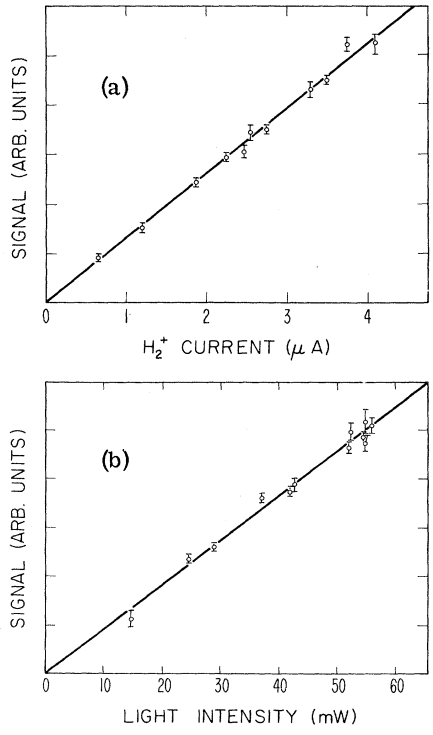

FIG. 3. Dependence of photodissociation signal upon (a) primary H_2^+ current and (b) bombarding light intensity.

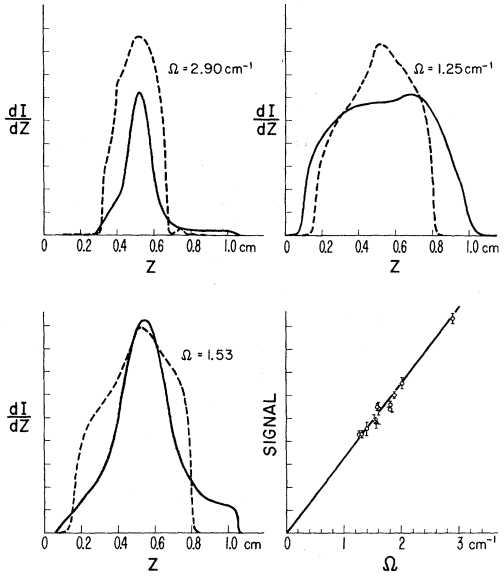

FIG. 4. Beam distribution functions as a function of spatial position Z. Solid curves show typical ion beam distribution curves $R(Z)$; dashed curves show photon distribution curves $G(Z)$. Values of the beam-overlap factor Ω are shown with each plot, and linearity of photodissociation signal with Ω is demonstrated in the lower right-hand plot.

Further evidence for the correct linearity with light power is provided by the fact that the measured cross section $\sigma(\lambda)$ forms a smooth curve despite strong and irregular variation of the light intensity over the spectrum. The proper dependence of the target density on the beam velocity v_i has been verified in electron-impact dissociation measurements by Dunn and Van Zyl.[20] Similarly, the present experiment shows the photodissociation cross section of H_2^+ at 3660 Å to be the same with 4- and 8.33-keV ions. Examples of beam profiles and the right functional connection between signal and overlap factor Ω are displayed in Fig. 4.

Absence of external modulation of the dc background was demonstrated since there was no measurable signal with the light off. Signals possibly caused by the light beam alone, e.g., through release of electrons from surfaces by ultraviolet photons, would be present both in the "ions-on" and "ions-off" mode in the data run and would drop out by subtraction. Thus, the points at the origins of the graphs in Fig. 3 are valid points, though they are not explicitly shown.

Finally, one has to look for mutual interactions of the beams other than the one under investigation. The light could release gas adsorbed on the light trap, thereby modulating the residual gas pressure which, in turn, would cause a modulation of the proton background from dissociative gas collisions. The combination of pump and volume of the vacuum

vessel responds to such a periodic gas source as an RC circuit does to an alternating current. Amplitude and phase of the spurious signal therefore depend upon the repetition rate of the light pulses. If the chopping frequency f is high compared to the reciprocal of the vacuum time constant (approx. 0.3 sec), it can be shown that the relative contribution of the background modulation to the signal varies as $1/f$, assuming constant gas desorption during a light pulse. A $1/f^2$ frequency dependence is predicted if the desorption varies linearly up and down in the light rhythm. Such a dependence would be expected if gas is released by heating of surfaces hit by the light, whereas photodesorption proper should provide a square-wave modulated gas source. Data taken at low (7 Hz) frequency do not differ within statistical limits from those obtained at 28 Hz.

The magnitude of the possible effect was further assessed as follows. A 170-mW beam of 3660-Å (3.4 eV) light was alternately turned on and off in a dc fashion, i.e., with a period of several seconds. This produced a static pressure increase of 3×10^{-12} Torr on a background of 6.3×10^{-10} Torr. The time constant and attenuation factor of the vacuum system were determined by observing the pressure fluctuations introduced by a modulated ion beam as the modulation frequency was varied between dc and several Hz. It was thus determined

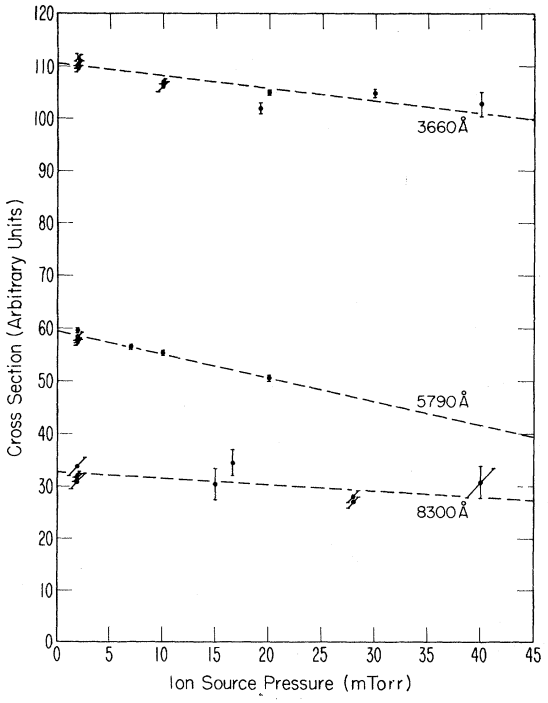

FIG. 5. H_2^+ photodissociation signal for three wavelengths as a function of pressure (mTorr) in the ion source where the H_2^+ are originally formed. Flags on the points indicate standard deviations.

that at this high photon power, the amplitude of the pressure modulation should have been about 4.5×10^{-14} Torr at 28 Hz if vacuum system filtering were the only filtering mechanism operating. This would account for about 5.4×10^{-17} A of modulated H^+ due to gas dissociation which, in turn, would be compared to about 4×10^{-14} A of signal H^+ at this wavelength and power level. This 0.1% effect would be detected as an even smaller one if we take into account the rather large (almost 90°) phase shift θ introduced by the vacuum-system filtering and the fact that the lock-in output is proportional to $\cos\theta$. If desorption by photons is a thermal effect, the amplitude is further reduced by $1/f$ and the further phase shift leads to a negative contribution to the cross section. As the latter effects cannot be verified, the larger uncertainty of 0.1% is attached to this process.

An unambiguous interpretation of the results of this experiment requires proof that collisional effects in the ion source do not influence the data. A strong variation of the measured cross section with ion-source pressure was found in a previous investigation of H_2^+ photodissociation.[5] This could not be confirmed in the present experiment. One has to recognize, though, that a physically different type of ion source (Penning type) was used in the earlier measurements. Figure 5 shows the dependence of the cross section on pressure in the ion source at 3660, 5790, and 8300 Å. Data are normally taken at a pressure of 2 mTorr, and one can see from the figure that only very small corrections are implied by extrapolation to zero pressure. All measurements at 2 mTorr, have been uniformly multiplied by 1.008 to account for this effect, and an 0.8% uncertainty has been allowed for due to the slight dubiosity of the correction. The difference in slopes of the sketched-in lines of Fig. 5 apparently indicates differences in cross sections for collisional deactivation from the vibrational levels principally involved at each wavelength. At 3660 Å the levels are mainly $v=6$ and 7; at 5790 Å, $v=8$ and 9; and at 8300 Å, $v=10$ and 11. In view of the limited amount of data, little more can be said on this point.

IV. RESULTS

Cross-section values calculated by putting experimentally measured quantities into Eq. (4) are shown as points in Figs. 6 and 7 for H_2^+ and D_2^+, respectively. The "interior" uncertainty flags indicate statistical uncertainty, and represent 90% confidence limits for the mean. Systematic uncertainties have been added linearly to the 90% confidence limits to give the "exterior" flags in the figure.

Each point represents averages of from 3 to 6 runs and of 25 to 40 measurements per run. Since

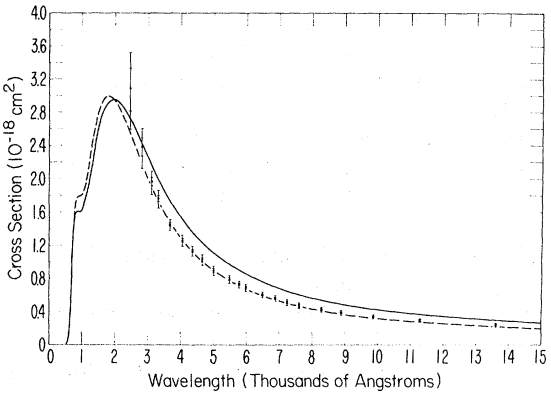

FIG. 6. Cross section in 10^{-18} cm^2 units for photodissociation of H_2^+ as a function of wavelength in thousands of angstroms. The points are experimental values, the interior flags show 90% confidence limits, and the exterior flags show maximum systematic uncertainties added to the 90% confidence limits. The solid curve is calculated from Eq. (3) using values for $\sigma_{v\mathcal{K}}(\lambda)$ from Ref. 6(c) and normalized Franck-Condon factors from Ref. 11 averaged over a thermal distribution for p_v (see Table II, column B). The dashed curve is similarly calculated except that p_v values are derived from Eq. (10) assuming a $Q_e(r)$ as in Eq. (12) (see Table II, column C).

each run is separately calibrated, variance[22] of the over-all average includes variance of the measurements and variance of the calibrations. The value of the student t function needed to obtain confidence limits is thus chosen on the basis of the number of *runs* rather than the number of *measurements*, since the variance in calibration generally was somewhat larger than the variance in measurements. However, variance in calibration was independent of ion species (H_2^+ or D_2^+) and independent of wavelengths above 5000 Å. It was thus possible to group runs of different species and different wavelengths to obtain the calibration variance and the value of the t function. Values of the t function used thus ranged from 1.90 at 2537 Å, where the least correlation was possible, to 1.67 for wavelengths greater than 5000 Å.

A small number of measurements were rejected. This was done when the deviation of the measurement from the mean of the run exceeded three times the standard deviation for a single measurement. Of 3209 measurements made in 101 runs with H_2^+, only 11 measurements were rejected on this basis. A pair of runs at 5461 and 3660 Å done on the same day were found to have measurement variances almost 10 times those of other runs at the same wavelengths. Examination of the distributions of measurement values showed broad flat distributions rather than the usual normal-appearing distritions. These entire runs were rejected, the data having been previously footnoted with the fact that highly microphonic conditions existed in the signal amplifier. Other than these cases, all data were accepted and averaged into the final values once the best instrumentation and procedures had been evolved.

Uncertainties other than purely statistical ones associated with accumulating data in the presence of noise are referred to here as systematic uncertainties. Sources of these uncertainties in cross sections are listed below, and assigned percentage values are indicated in parentheses. Some values cited cover a range and depend on wavelength. Except where specifically noted, uncertainties were assessed by careful measurements:

(a) transmission of final three optical elements (± 2.0–± 5.0);

(b) absolute determination of effective wavelength (± 0.05–± 0.8);

(c) residual scattered visible light (only in data at 2537 Å) (± 0.05);

(d) calorimeter constant (± 0.5);

(e) beam overlap, determination of C, in Eq. (4) ($+0, -0.5$);

(f) beam overlap, correction for slightly nonlinear probe drive (± 0.1);

(g) beam overlap, choice of base line in numerical overlap integrals (± 0.5);

(h) beam overlap, constancy and reproducibility (± 1.0);

(i) ion velocity (± 0.2);

(j) ion collection efficiency ($+0, -0.5$);

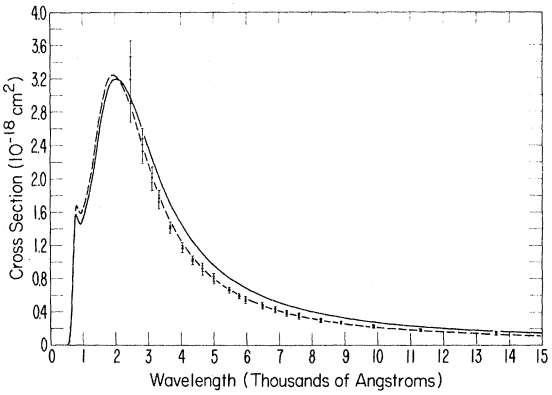

FIG. 7. Cross section in 10^{-18} cm^2 units for photodissociation of D_2^+ as a function of wavelength in thousands of angstroms. The points are experimental values, the interior flags show 90% confidence limits, and the exterior flags show maximum systematic uncertainties added to the 90% confidence limits. The solid curve is calculated from Eq. (3) using values for $\sigma_{v\mathcal{K}}(\lambda)$ from Ref. 6(c) and normalized Franck-Condon factors from Ref. 11 averaged over a thermal distribution for p_v (see Table II, column B). The dashed curve is similarly calculated except that p_v values are derived from Eq. (10) assuming a $Q_e(r)$ as in Eq. (12) (see Table II, column C).

TABLE I. Measured photodissociation cross sections of H_2^+ and D_2^+ at various effective wavelengths along with 90% statistical confidence limits and maximum systematic uncertainties.

Wavelength λ_e(Å)	Cross section σ (10^{-19} cm^2)	90% confidence (±%)	Maximum systematic (+%)	(−%)
	H_2^+			
2472	30.7	8.2	5.9	7.1
2830	23.8	4.4	5.0	6.1
3116	19.6	2.4	3.9	5.1
3326	17.6	1.9	3.5	4.6
3669	14.5	1.0	3.1	4.2
4050	12.6	1.4	3.1	4.2
4360	11.3	1.3	3.1	4.2
4659	10.2	2.1	3.2	4.4
4998	8.97	1.9	3.2	4.4
5474	7.93	1.8	3.1	4.2
5784	7.27	1.0	3.1	4.2
5994	6.88	2.1	3.1	4.3
6496	6.03	1.5	3.2	4.4
6889	5.56	2.4	3.1	4.3
7242	5.11	2.7	3.1	4.3
7614	4.69	2.2	3.1	4.3
8282	4.25	2.2	3.1	4.3
8893	3.84	2.6	3.1	4.3
9880	3.37	1.9	3.2	4.4
11297	2.91	3.4	3.2	4.4
13613	2.34	4.5	3.6	4.8
	D_2^+			
2472	31.9	8.8	5.9	7.1
2830	24.1	3.0	5.0	6.1
3116	20.1	2.6	3.9	5.1
3326	17.6	2.3	3.5	4.6
3669	14.2	0.9	3.1	4.2
4050	11.8	1.5	3.1	4.2
4360	10.3	1.2	3.1	4.2
4659	9.19	3.8	3.2	4.4
4998	7.99	3.7	3.2	4.4
5474	6.65	1.2	3.1	4.2
5784	5.92	1.3	3.1	4.2
5994	5.47	3.5	3.1	4.3
6496	4.79	4.0	3.2	4.4
6889	4.29	4.5	3.1	4.3
7242	3.90	4.0	3.1	4.3
7614	3.56	5.4	3.1	4.3
8282	3.01	4.1	3.1	4.3
8893	2.71	3.4	3.1	4.3
9880	2.31	3.1	3.2	4.4
11297	1.87	4.3	3.2	4.4
13613	1.48	6.7	3.6	4.8

(k) modulation by light beam of background gas (± 0.1);

(l) ion-source pressure dependence (± 0.8);

(m) calibration of 10^{10}-Ω signal input resistor (± 0.2);

(n) temperature drift of signal input resistor (+ 0.33, − 0.15);

(o) calibration of input amplifier (± 0.2);

(p) scale ratios of input amplifier (± 0.2);

(q) scale ratios of lock-in detector (± 0.05 to ± 0.7);

(r) nonlinearity of input amplifier (± 0.3);

(s) modulation of calibration ion beam for signal channel compared to light modulated signal (+ 0, − 0.5);

(t) calibration resistor for ion beam channel (± 0.1, manufacturer's value);

(u) calibration voltage for ion beam channel (+ 0.15, − 0).

These uncertainties were combined as follows. To the sum of the squares of the *uncorrelated* ones was added the square of the sum of the *possibly correlated* ones [(o)–(q) and (t) may be temperature correlated]. To the square root of this sum were added linearly the asymmetric uncertainties [(e), (j), (n), (s), and (u)]. These results are termed the maximum systematic uncertainties of the cross-section values at the given wavelength.

Experimental cross-section values together with 90% confidence limits and maximum systematic uncertainties are listed in Table I for both H_2^+ and D_2^+ for all 21 values of effective wavelength at which measurements were made.

V. INTERPRETATION AND DISCUSSION

A. General

The solid curves in Figs. 6 and 7 give photodissociation cross sections as a function of wavelength for H_2^+ and D_2^+, respectively, as calculated from Eq. (3) using $\sigma_{v\mathcal{K}}(\lambda)$ given by Dunn[6(c)] and assuming the p_v are normalized Franck-Condon factors connecting the ground vibrational state of the molecule with the ion. The significant differences between measured values and computed curves suggest that Franck-Condon factors do not adequately describe populations of vibrational levels of the target ions.

Since Eq. (3) is valid at all n wavelengths λ_j investigated experimentally, we have a system of n equations

$$\sigma(\lambda_j) = \sum_v p_v \sigma_{v\mathcal{K}}(\lambda_j) \qquad (6)$$

in the unknown p_v. Here $\sigma(\lambda_j)$ are the experimentally determined values and the $\sigma_{v\mathcal{K}}(\lambda_j)$ are theoretical.[6(c)] Unfortunately, for many v's the coefficients $\sigma_{v\mathcal{K}}(\lambda_j)$ are zero or very small for experimentally accessible wavelengths, and the system of equations thus offers an incomplete opportunity to solve for all the p_v's. At a given λ_j most of the contribution to $\sigma(\lambda_j)$ comes from only a few levels v. For example, at 6000 Å for H_2^+, approximately 57% of the contribution to photodissociation comes from $v=8$, 18% from $v=7$, and 15% from $v=10$. This fact enhances the uniqueness of the solution for the p_v's despite the incompleteness of the data for all p_v's noted above.

A least-squares fit of the data to Eq. (6) will thus yield rather unique values for some of the p_v's.

TABLE II. Populations for H_2^+ and D_2^+ for various vibrational quantum numbers v. (A) Populations derived from least-squares fit of photodissociation cross-section data to Eq. (6) (underlined numbers result from the fit, others were entered into the equation); (B) normalized Franck-Condon factors (Ref. 11) averaged over a Boltzmann distribution at 100 °C; (C) populations computed from Eq. (10) assuming a variation with r of the electronic matrix element according to Eq. (12).

v	(A)	(B)	(C)
		H_2^+	
0	0.119	0.092 02	0.119 16
1	0.190	0.162 12	0.189 94
2	0.188	0.176 34	0.187 91
3	0.152	0.154 74	0.151 73
4	0.125	0.121 17	0.110 97
5	0.075	0.089 01	0.077 32
6	0.052	0.063 19	0.052 70
7	0.037	0.044 02	0.035 64
8	0.024	0.030 47	0.024 11
9	0.016	0.021 10	0.016 38
10	0.011 7	0.014 67	0.011 21
11	0.008 2	0.010 25	0.007 73
12	0.005 7	0.007 21	0.005 36
13	0.003 74	0.005 08	0.003 74
14	0.002 58	0.003 55	0.002 58
15	0.001 75	0.002 42	0.001 75
16	0.001 09	0.001 55	0.001 09
17	0.000 56	0.000 83	0.000 56
18	0.000 12	0.000 23	0.000 12
		D_2^+	
0	0.044 8	0.034 26	0.044 78
1	0.103 8	0.085 47	0.103 77
2	0.140 7	0.124 12	0.140 70
3	0.147 6	0.138 39	0.147 65
4	0.133 7	0.132 05	0.133 74
5	0.110 6	0.114 16	0.110 59
6	0.085	0.092 38	0.086 24
7	0.063	0.071 56	0.064 70
8	0.042	0.053 83	0.047 36
9	0.034	0.039 73	0.034 13
10	0.024	0.028 99	0.024 40
11	0.017	0.021 04	0.017 39
12	0.012 2	0.015 24	0.012 41
13	0.008 8	0.110 6	0.008 89
14	0.006 4	0.008 05	0.006 41
15	0.004 8	0.005 89	0.004 65
16	0.003 6	0.004 33	0.003 40
17	0.002 50	0.003 20	0.002 50
18	0.001 85	0.002 38	0.001 85
19	0.001 38	0.001 78	0.001 38
20	0.001 02	0.001 32	0.001 02
21	0.000 75	0.000 98	0.000 75
22	0.000 54	0.000 72	0.000 54
23	0.000 37	0.000 50	0.000 37
24	0.000 23	0.000 32	0.000 23
25	0.000 11	0.000 16	0.000 11
26	0.000 02	0.000 04	0.000 02

Before a meaningful fit can be computed, values p_v^a are assumed (e.g., taken from Franck-Condon predictions) for those levels that make only a small contribution to the sum over the whole range of wavelengths covered by our data. These contributions are then subtracted from the measured cross section. This procedure reduces the order of the computational problem and enables us to obtain fitted values for the remaining p_v's. The fitted values obtained depend only very weakly on the assumed values p_v^a, as discussed quantitatively below, and after obtaining one set of p_v's, new p_v^a's may be chosen by requiring that a plot of p_v vs v should be a smooth curve of not too different character from Franck-Condon values. The fitting procedure can then be repeated with the new p_v^a's.

Such a solution of the system for the p_v's with $v=4-12$ for H_2^+ and $v=6-16$ for D_2^+ produces values underlined in column A of Table II. The entries in this column without underlines (for $v=0-3$, 13–18 for H_2^+, and $v=0-5$, 17–26 for D_2^+) are values p_v^a used in the fit procedure, but whose magnitudes have very little effect on the outcome of the fits. Thus, if values of p_v^a are taken from column B of Table II rather than column C, as was done, we get p_v values which are -0.6%, $+0.2\%$, -0.1%, -0.05%, $+0.2\%$, -0.3%, -2.3%, -1.1%, and -8% different from the values quoted in column A for $v=4-12$, respectively, for H_2^+.

Column B of Table II lists normalized Franck-Condon factors averaged over a thermal distribution of rotational levels of the parent neutral molecule assumed at 100 °C, and assuming no rotational excitation occurs in the ionizing collision. The Franck-Condon factors of Villarejo[11] for the various K'', K' values involved have been used in obtaining this average. These values were used to obtain the solid curves of Figs. 6 and 7.

Column C of Table II lists p_v values derived assuming a variation with internuclear separation of the electronic matrix element involved in electron-impact ionization of the neutral molecule. This will be discussed in detail in Sec. V D. The p_v values in column C were used in Eq. (3) to obtain the dashed curves in Figs. 6 and 7.

As we look for reasons for the differences between measured and calculated cross sections shown in Figs. 6 and 7 and between fitted and calculated p_v's shown in Table II, several possibilities present themselves: (a) Rotational excitation in the ionizing collision may be very prevalent and, owing to the dependence of Franck-Condon factors on rotation, may thus alter the populations of the v' levels of the ion. (b) If ionization proceeds via autoionization, the populations of resultant v' levels of the ion are not likely to be the same as in direct ionization, the process which has been assumed. (c) If the electronic matrix element involved in direct elec-

tron-impact ionization varies with internuclear separation, then one does not expect the populations to be given by simple Franck-Condon factors. These possibilities are discussed in more detail below. They are examined separately and independently, though it must be recognized that some combination of these effects may represent reality.

B. Rotational Effects

We examine first the possibility that rotational excitation in ionizing collisions has a significant effect on the populations p_v'. A Boltzmann distribution is assumed for the initial rotational levels of the parent molecule:

$$n(K'') = (2K''+1) g_{K''} \exp[-B_v K''(K''+1)/kT] ,$$

where B_v is the rotational constant for vibrational level v of the molecule, k the Boltzmann constant, T the temperature taken as 373 °K, and $g_{K''}$ is a statistical weight factor, which for H_2 is 1 for K'' even and 3 for K'' odd. Values of $n(K'')$ for $K'' \geq 4(5)$ add up to only 1.2(4)% for H_2 (D_2) and have been set at zero, since Franck-Condon factors have not been calculated for these higher rotational levels.

We further assume that the probability for a transition from the $v''K''$ level of the neutral to the $v'K'$ level of the ion is proportional to the relevant Franck-Condon factor $q(v', K'; v''K'')$ and to a factor which governs rotational excitation $F(K', K'')$. The factor $F(K', K'')$ must vanish for odd values of $|K' - K''|$, since the ortho-para character of the molecule is maintained in an ionizing transition to the ground electronic state of the ion. For ionization by high-energy electrons it is likely that changes in K are equally probable in either direction, so we assume that $F(K', K'')$ has the character $F(|K' - K''|)$. With these assumptions, we have for the population factors

$$p_{v'K'} = \frac{1}{\sum_{K''} n(K'')} \sum_{K''} \frac{n(K'')(2K'+1) q(v', K'; 0, K'') F(|K' - K''|)}{\sum_K (2K+1) F(|K - K''|) \sum_{v'} q(v', K; 0, K'')} . \quad (7)$$

We have evaluated Eq. (7) assuming that $F(0) = 1$ and treating $F(2)$ as a parameter, with $F(4)$ and values of F for higher $|K' - K''|$ taken as 0. Values of $F(2)$ have been varied between 0 and 0.25, and the resultant $p_{v'} = \sum_{K'} p_{v'K'}$ show only a modest dependence on $F(2)$. Column B of Table II lists $p_{v'}$ for $F(2) = 0$. In Fig. 8 are plotted the ratios of $p_{v'}$ for $F(2) = 0.1$ and 0.25 to $p_{v'}^0$, the value for $F(2) = 0$, as a function of v'. Also plotted for comparison are the ratios $p_{v'}/p_{v'}^0$, where the $p_{v'}$ have been obtained from column C of Table II. We see that the changes in $p_{v'}$ brought about by possible rotational excitation are of a much different magnitude and a dramatically different character than experimentally deduced.

There is strong evidence[23] in the case of ionization of N_2 by electrons that the rotational temperature does not change. If this can be transferred[24] to H_2, then it is reasonable that all $F(|K' - K''|)$ except $F(0)$ are small, further supporting the contention that rotational effects are not significant here in changing the p_v.

Before leaving the discussion of rotational and temperature effects, a few final observations are in order. First, the ion-source temperature is nonuniform, as noted in Sec. III B. This should make very little difference as long as rotational excitation upon ionization is small, since Villarejo's diagonal Franck-Condon factors are essentially identical. Rotational excitation—as already observed—leads to p_v changes in a different direction and of a smaller magnitude than observed. Second, the hot filament which subtends a small but finite solid angle to the ion-forming volume in the ion source was ignored in assessing the temperature. It is thus possible that a small number of parent gas molecules are vibrationally as well as rotationally excited. The normalized Franck-Condon factors in Table III between the (1, 0) state of H_2 and the $(v, 0)$ state of H_2^+, however, show that this too would produce an effect in the opposite direction to the observations. The entries in Table III were computed using the same technique as in Ref. 10, except that the ground-state H_2 curve of Kolos and Wolniewicz[25] was used.

C. Autoionization

If the neutral molecule is excited to the $v'''K'''$ level of a Rydberg state this state can, in some cases, autoionize to the $v'K'$ state of the ion. Thus we may have

$$H_2(^1\Sigma_g^+, v'', K'') + e \rightarrow H_2^*(R, v''', K''') + e$$

followed by

$$H_2^*(R, v''', K''') \rightarrow H_2^+(^2\Sigma_g^+, v', K') + e .$$

A Rydberg state R is schematically shown in Fig. 1. We note that it is necessary to convert internal vibration-rotation energy into electronic energy for this process to go. Similarly, we note that normally $v' < v'''$.

Autoionization of Rydberg states of H_2 was recog-

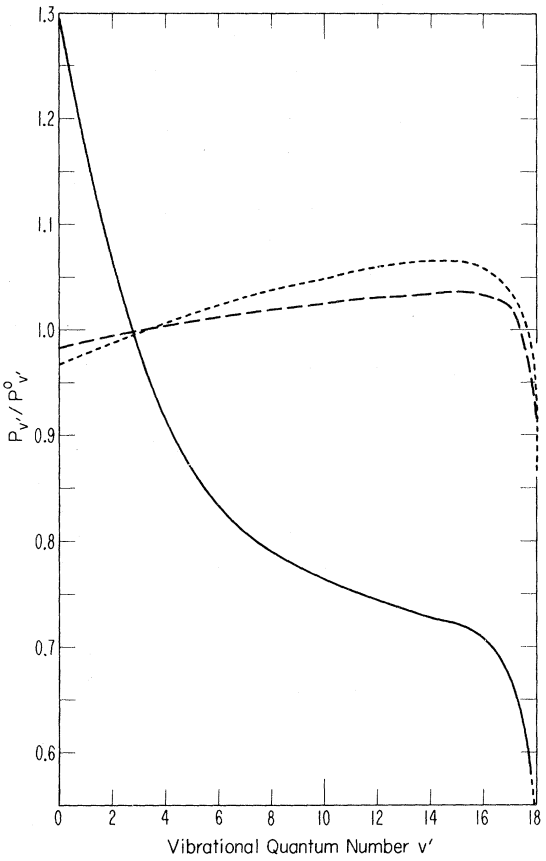

FIG. 8. Plot of $p_{v'}/p^0_{v'}$ for H_2^+ as a function of vibrational quantum number v'. For the dotted and dashed curves, $p_{v'}=\sum_{K'} p_{v'K'}$ were computed using Eq. (7). The dotted curve is for $F(2)=0.25$ (20% rotational excitation upon ionization to the $K'=2$ state) and the dashed curve is for $F(2)=0.1$ (9% rotational excitation). The populations $p^0_{v'}$ were calculated assuming $F(2)=0$. For the solid curve, $p_{v'}$ was computed from Eq. (10) with $Q_e(r)$ given by Eq. (12) (see Table II, column C).

nized spectroscopically by Beutler and Jünger[26] and more recently studied by a number of others.[15,17,27–31] Dibeler *et al.*,[28] in their study, proposed breakdown of the Born-Oppenheimer separation as the means of coupling internuclear to electron motion. This concept was developed by Berry,[32] and subsequent theoretical work has been done by others.[33–36] The classic work of Chupka and Berkowitz[17] illustrates the process in detail, verifies many of the general theoretical predictions, and points out limitations on the present theories.

Several electron-impact studies of ionization and autoionization are particularly relevant to this work. Briglia and Rapp[37] observed a near-linear ionization cross section for ionization of H_2 near threshold as opposed to a series of linear segments with incremental slopes in the ratio of the Franck-Condon factors, as previously observed by Marmet and Kerwin.[38] They suggested the departure from the Franck-Condon model was due to autoionization of the type discussed above. McGowan and coworkers[24,39] observed structure in the derivative of the cross section for electron-impact ionization of H_2 which they correlated with autoionization through photoionization studies.[27,28] In their later paper[39] McGowan *et al.* carried out a data analysis to get the fraction of ions formed by autoionization versus the direct process as a function of electron energy. Their procedure was to match the slope of the ionization efficiency curve derived from the Franck-Condon model to their experimental results at 3.0 eV above threshold. Results of their observations and analysis, shown in Fig. 2 of their paper, indicate that about 80% of ions near threshold are formed by autoionization. This decreases to about 40% at 2 eV above threshold, and one extrapolates the curve to give near-zero contribution from autoionization by a few tens of electron volts electron energy. To a large extent, the steeply decreasing fraction of autoionization is "built in" to their conclusions by their slope-matching procedure. This was prompted by their feeling that it is not "physically realistic" for autoionization to continue as a strong contributor to ionization at higher electron energies. Though this assumption and analysis may be correct, it is not unique nor conclusive enough to allow us to ignore autoionization here.

If one independently considers that autoionization occurs as a result of electron-impact excitation of the neutral, and that many electron-impact excitation curves rise and fall with electron energy in a manner not too dissimilar to ionization, then it is

TABLE III. Normalized Franck-Condon factors for the transition $H_2(^1\Sigma_g^+;\ v''=1,\ K''=0) \rightarrow H_2^+(^2\Sigma_g^+;\ v',\ K''=0)$.

v'	$p_{v'}$
0	0.368
1	0.210
2	0.0428
3	0.000
4	0.0178
5	0.0418
6	0.0541
7	0.0550
8	0.0494
9	0.0414
10	0.0331
11	0.0258
12	0.0197
13	0.0148
14	0.0108
15	0.0076
16	0.0049
17	0.0026
18	0.0006

not unreasonable that autoionization could be a contributing channel for ion formation at high as well as low electron energies. In particular, ion formation by this channel may be important for electron energies used in this experiment.

If this were the case, the population distribution in vibrational levels of the ion might be quite different from Franck-Condon and, of course, might be the reason for the discrepancy of our photodissociation data with the "predicted" values. It is therefore reasonable to consider what one might expect. Only a very oversimplified picture will be examined.

Suppose that all autoionization can be considered to originate from an equivalent single Rydberg state R, and that this state lies very close to the ion so that its shape is nearly identical. The latter condition makes the Franck-Condon factors for excitation to the Rydberg level essentially the same as those for ionization. Suppose, further, that the vibration propensity rule in autoionization $\Delta v = -1$, proposed in theoretical treatments[32–35] and largely confirmed by Chupka and Berkowitz,[17] holds rigorously. Then we have

$$p_v = D\mathcal{P}_v + A\mathcal{P}_{v+1} \ , \tag{8}$$

where p_v is the resultant population of the v level of the ion, $\mathcal{P}_v$ is the normalized Franck-Condon factor to either the ion or state R, D is the fraction of ions formed by the direct channel, and A is the fraction formed by autoionization. Assume $A + D = 1$ and ignore interference between the two channels.

Since for the range of v we have probed experimentally with the wavelengths available, $\mathcal{P}_{v+1} < \mathcal{P}_v$, the effect of autoionization is to lower p_v from the earlier assumed $\mathcal{P}_v$ towards $\mathcal{P}_{v+1}$. This is the direction of the effect observed experimentally. By using the normalization on A and D to eliminate D in Eq. (8) we can solve for A:

$$A = (\mathcal{P}_v - p_v)/(\mathcal{P}_v - \mathcal{P}_{v+1}) \ . \tag{9}$$

Substituting values for p_v from column A of Table II and values of $\mathcal{P}_v$ and $\mathcal{P}_{v+1}$ from column B, we can solve for the necessary fraction of ions formed via autoionization if our data are to be explained in this fashion. One finds that, on the average, 64% of the H_2^+ ions and 65% of the D_2^+ ions must be formed by autoionization if our photodissociation data are to be explained by the above model.

Despite the apparent ability to account qualitatively for the observations in this experiment, there are some facts which bring about gnawing doubts about its full applicability here. The possible conflict with McGowan *et al.*[39] has already been mentioned, though as noted this was not sufficient by itself to rule out autoionization. Further, the nearly $\frac{2}{3}$ fraction of ions formed by autoionization in order for this model to work would mean that the peak cross section[40] for direct ionization of H_2 is only about 0.36×10^{-16} cm^2. This would be only about half the value for ionization of the single H atom, 0.7×10^{-16} cm^2! There seem to be no quantum calculations for H_2 ionization, but semiclassical calculations[41] for direct ionization of H_2 are in quite good agreement (~20%) with experiment. If the simple model and analysis here are correct, making $\frac{2}{3}$ of the experimental value arise from autoionization, then the semiclassical calculations are off by about a factor of 3. This does not seem consistent with the success of semiclassical methods in calculating ionization for atoms and other molecules.

In addition, the fractional value of autoionization A needed for the model is essentially the same for H_2 and D_2. It has already been pointed out that molecular autoionization depends upon coupling vibrational motion to electronic motion, and computed rates have been found[33] to have a strong isotope effect. Clearly, this is something not consistent with the demands of the model to explain our data—unless the rate for autoionization is so high compared to other decay modes (predissociation and radiation) that the difference in rate does not matter. Again, however, computed predissociation rates[33] compete quite strongly with autoionization, and with a sizeable isotope dependence.

In view of the several difficulties encountered with the autoionization model for explaining our data, we tend to discount—though not entirely reject—this interpretation.

D. Electronic Matrix Element for Electron-Impact Ionization of H_2

The elementary form of the Franck-Condon principle normally used, and used here in the discussion of the ion-forming process to this point, assumes that the electronic transition matrix element varies slowly enough with internuclear separation that it can be factored out of the integration over that variable. This leaves simply the overlap squared of the vibrational wave functions to determine the relative transition strengths to various vibrational levels. More correctly, we have

$$p_{v'} = \frac{|\int \chi_{0K''}(r)\, Q_e(r)\, \chi_{v'K'}(r)\, dr|^2}{\sum_v |\int \chi_{0K''}(r)\, Q_e(r)\, \chi_{vK'}(r) dr|^2} \ . \tag{10}$$

It should not be surprising if $Q_e(r)$ varies fast enough with r to make a significant contribution in Eq. (10). Flannery and Öpik[42] have calculated the equivalent matrix elements for photoionization of H_2, and they find that the dependence on r is significant and different for different wavelengths as well as depending on whether perpendicular or parallel transitions are involved. One might expect in our problem that whatever $Q_e(r)$ satisfies the

data for H_2 should also satisfy the data for D_2.

We have sought by successive trials for such a $Q_e(r)$ using the criterion that the quantity $T^2 < 1$, where

$$T^2 = \frac{\sum_\lambda (\Delta\sigma_\lambda)^2/S_\lambda^2}{n-1}, \tag{11}$$

if we are to claim agreement with experiment. Here $\Delta\sigma_\lambda = \sigma(\lambda)_{\text{expt}} - \sigma(\lambda)_{\text{calc}}$, n is the number of wavelengths at which observations were made, and S_λ^2 is the sum of the squares of the statistical and systematic uncertainties in $\sigma(\lambda)_{\text{expt}}$. The quantities $\sigma(\lambda)_{\text{expt}}$ and $\sigma(\lambda)_{\text{calc}}$ are, respectively, the experimental values and the values computed from Eq. (3) using p_v, from Eq. (10) with an assumed $Q_e(r)$ and wave functions as in Ref. 10, except that the ground-state H_2 potential of Kolos and Wolniewicz[25] was used.

It was found that the function

$$Q_e(r) = 1 + 0.56(r_{\text{a.u.}} - 0.99)^2 \quad \text{for } 1 \leq r_{\text{a.u.}} \leq 2 \tag{12}$$

satisfied the criterion on T^2 for both H_2 and D_2. Values of p_v from Eq. (10) using Eq. (12) are listed in column C of Table II. The dashed curves in Figs. 6 and 7 are from Eq. (3) using these values of p_v.

Thus, a fairly simple function with a not unreasonably large variation with r can explain our photodissociation data. It must be emphasized, however, that Eq. (12) does not necessarily represent a unique $Q_e(r)$, and no optimizing procedures have been used in arriving at $Q_e(r)$—except that successive trials have brought the authors to a local optimum under the criterion of Eq. (11). Similarly, $Q_e(r)$ is given in an arbitrary system of units, and normalization of the p_v is achieved by Eq. (10).

VI. RELATIONSHIP OF RESULTS TO OTHER EXPERIMENTS

A. Photoelectron Spectroscopy

During the past few years a number of workers have published[43] photoelectron spectra from H_2 ionization primarily using 584-Å He resonance radiation. Generally, these spectra distinctly show the peaks corresponding to each vibrational level of H_2^+, and the peak heights should be related to the relative Franck-Condon factors. Interpretation of the data is complicated by uncertain relative transmission functions of the various spectrometers, but, typically, the data are in reasonable agreement with simple Franck-Condon factors such as those given in column B of Table II. Indeed, one expects this of a good experiment in this case, since near 584 Å the matrix elements calculated by Flannery and Öpik[42] are flat with r, and since it is a short enough wavelength that autoionization should no longer be important. There is thus no conflict of these experiments with the results and possible interpretations of the present experiment.

Villarejo[44] measured threshold electrons in photoionization of H_2 and D_2 at a variety of wavelengths and did not get good agreement with a Franck-Condon model.

Penning electron spectra[45] from Penning ionization of H_2 by He and Ne metastables show a lower population of higher vibrational levels and a higher population of the low ones—much as is observed in the present experiment. However, again we recognize that the ion-forming process is a different mechanism and there is neither conflict nor confirmation as far as the present measurements are concerned.

B. Electron-Impact Dissociation of H_2^+

Cross-section measurements for proton production (excitation plus twice ionization cross sections) by electron impact on H_2^+ have been reported by Dunn and Van Zyl[20] and by Dance *et al.*[46] Recently, Peart and Dolder[47] have measured the excitation cross section and the excitation plus the ionization cross section. Interpretation of the experiments[20,46] was similar to that of the present measurement, and an equation analogous to Eq. (3) was employed using Franck-Condon factors for the p_v and calculations by Peek[48] for cross sections from individual levels. Agreement with theory can be considered quite good for all experiments, and agreement among the experiments is good, especially at high energies.

Since the experiment of Dunn and Van Zyl was done with the same ion source as used in the present measurement, it is well to consider whether the mentioned agreement is impaired or improved by changing the p_v from Franck-Condon factors to the deduced ones of the present paper. Figure 9 shows the results of such a query. Here the cross section multiplied by electron energy is plotted versus log of electron energy. The solid line is obtained using Franck-Condon factors of column B of Table II for p_v in the analog of Eq. (3); the dashed line is obtained using p_v from column C of Table II.

Experimental points of Dunn and Van Zyl[20] and Dance *et al.*[46] are also shown. The uncertainty flags show 90% confidence limits linearly added to stated maximum systematic uncertainty. Within these uncertainties, and if one in addition recognizes some uncertainty in the theoretical value of Peek,[48] there cannot be a rational judgment of the superiority of one set of p_v's over the other. Electron impact is not so sensitive as photon impact to the p_v's, and there is more uncertainty in the quantities to compare for electron impact. Similar conclusions are reached considering the unpublished data of Peart and Dolder.

Caudano and Delfosse[49] have measured the energy

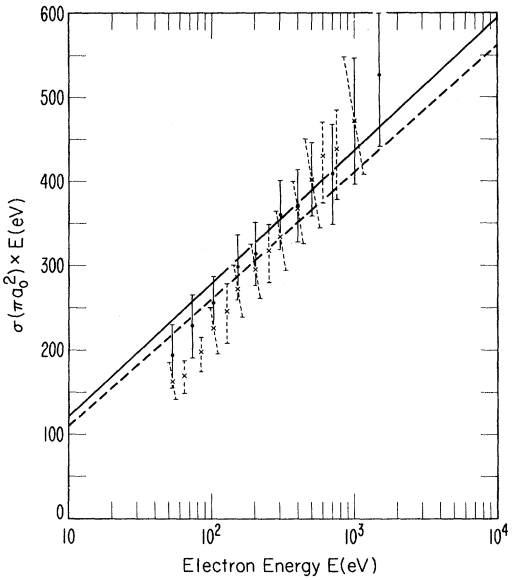

FIG. 9. Cross section multiplied by energy vs energy for electron-impact dissociation of H_2^+. The solid curve uses the theoretical cross sections of Peek (Ref. 48) and normalized Franck-Condon factors from Table II, column B for $p_{v'}$. The dashed curve also uses the cross sections of Peek and uses $p_{v'}$ from Eq. (10) assuming $Q_e(r)$ as in Eq. (12) (see Table II, column C). Points are the data of Dunn and Van Zyl (Ref. 20) and crosses are the data of Dance *et al.* (Ref. 46). Uncertainties are 90% confidence limits added linearly to maximum systematic errors.

distribution of protons from electron-impact dissociation of H_2^+. The analysis of these data by Peek and Green[50] shows better agreement between experiment and theory using the p_v deduced in the present experiment as compared to using Franck-Condon factors—though neither set of p_v's yields satisfactory agreement. These authors,[49] however, used a Penning ion source, and it may be that their results are not interpretable in terms of the p_v resulting from simple high-energy electron impact on H_2.

C. Other Experiments

There are a number of other experiments on which this work has some bearing. It is not reasonable to discuss them all in detail here, but it is appropriate to make brief reference to some of them.

The relationship to electron-impact ionization experiments on H_2 has been mentioned in Sec. V, and will not be pursued here. The results and interpretations of Sec. V have rather definite implications about dissociative ionization of H_2 to the $1s\sigma_g$ state of H_2^+. The present work would imply a lower fraction of dissociative ionization than Franck-Condon predictions give. This question probably deserves further experimental investigation, since the measurements of Bauer and Beach[51] and Schaeffer and Hastings[52] probably suffered from velocity discrimination effects, and their measurements at 30 eV probably[53] included protons from the $2p\sigma_u$ state.

It is interesting—though perhaps not significant—that the electric field dissociation measurements of Riviere and Sweetman[54] are almost in exact agreement with the value of $p_{17}+p_{18}$ deduced in Sec. V D. Interpretation of many experiments[55] on the breakup of H_2^+ by collision with a gas may be affected by the p_v's deduced in this paper. Caution must be exercised, however, since in many of these studies discharge-type sources were used.

It was perceived that photodissociation measurements in conjunction with theory as used in this paper could also be used to deduce vibrational-state populations of H_2^+ formed from other molecules such as H_2O, NH_3, H_2S, etc. Such a measurement could be used to help distinguish various models for electron-impact ionization of such polyatomic molecules. For example, is the ionization a knock-on collision taking place rapidly enough that one would expect a v' distribution in the H_2^+ characteristic of the proton separation in the original molecule (essentially a Franck-Condon transition), or is a complex formed that lives long enough to redistribute the nuclei and thus alter the resultant v' distribution? Muschlitz computed various expected v' distributions on the basis of a variation of the Franck-Condon picture. Some measurements were made of photodissociation cross sections at a few isolated wavelengths using H_2^+ from NH_3 and from H_2O. Unfortunately, ion intensities were very low and the data were difficult to take, and in the time available for this effort no conclusive results were obtained.

VII. CONCLUSIONS

The photodissociation cross sections reported here remove the gross discrepancies between experiment and theory previously[5,6] found. Remaining differences between theory and experiment can be explained by a difference in the ion vibrational-state populations from those predicted with a simple Franck-Condon model for ionization. A set of populations of the levels v' has been deduced and tabulated, and they show a systematic deviation from normalized Franck-Condon factors. The difference can be explained by either of two models: (a) If about $\frac{2}{3}$ of all ions formed by electron impact at the energies of this experiment (~128 eV) are formed by autoionization, then vibrational-state populations consistent with those deduced in this work may result. (b) A variation with internuclear separation of the electronic matrix element for electron-impact ionization of H_2 and D_2 which goes according

to Eq. (12) will lead to populations consistent with the photodissociation data. A number of considerations lead us to favor the second explanation over the first, but this is by no means conclusive. It is possible—and perhaps even probable—that a combination of (a) and (b) is operative in leading to the populations deduced here.

The deduced populations are alleged to be those characteristic of high-energy electron-impact ionization of H_2 and D_2.

The results and interpretations are consistent with other relevant experiments. A number of experiments should be reinterpreted with the newly deduced populations.

ACKNOWLEDGMENTS

The authors are pleased to acknowledge the close collaboration in the early stages of the experiment of Dr. Bert Van Zyl, who co-authored a report of preliminary data (see Ref. 56). They are also grateful for help and collaboration of Dr. E. E. Muschlitz in some late phases of the work. They thank Dr. Brian Joiner, who was most helpful with discussions and advice on statistical interpretation of the data, and Dr. Bruce Steiner, who loaned the large grating for use in the infrared. Many colleagues and visitors at JILA also contributed to our understanding of the problems involved.

APPENDIX

In arriving at Eq. (3) from Eq. (2) it was assumed that $\sigma_{vK}(\lambda) \approx \sigma_{v\mathcal{K}}(\lambda)$, where $\mathcal{K}$ is an effective rotational quantum number such that

$$\sigma(\lambda) = \sum_v \sum_K p_{vK}\, \sigma_{vK}(\lambda) = \sum_v \sigma_{v\mathcal{K}}(\lambda) \sum_K p_{vK} \,. \qquad \text{(A1)}$$

We proceed now to discuss the error involved in this approximation.

Rotation adds the same centrifugal term to both $V_g(r)$ and $V_u(r)$, the potentials for the $1s\sigma_g$ and $2p\sigma_u$ states of the ion, respectively. The energy of the bound states is shifted so that

$$E_{vk} = E_{v0} + B_v K(K+1) \,,$$

and the nodes of the bound-state vibrational wave functions are shifted by an amount which, according to Villarejo,[11] is $\Delta r(K) = \alpha r_0 K(K+1)$. Here r_0 is the position for $K=0$ and α is a slowly varying function of r with a magnitude about 6×10^{-4} for H_2^+ and 3×10^{-4} for D_2^+. So we make the approximation $\chi_{vK}(r) \simeq \chi_{v0}[r - \Delta r(K)]$. Similarly, the continuum wave functions are shifted in r upon addition of the centrifugal term. These functions are also shifted by small changes in k, the wave number of dissociating particles, and one can express small changes in r as equivalent small changes in k.

Using these approximations for wave functions in Eqs. (14) and (15) of Ref. 6(b), it can be shown that approximately

$$\sigma_{vK}(\nu) = (1 + A + \Delta\nu/\nu)\, \sigma^A_{v\mathcal{K}}(\nu - \Delta\nu) \,, \qquad \text{(A2)}$$

where

$$A = [K(K+1) - \mathcal{K}(\mathcal{K}+1)] \left(2\alpha r_0 \frac{1}{Q_e} \frac{dQ_e}{dr} - \frac{1}{2k^2} \langle r^{-2} \rangle_v \right)$$

and

$$\frac{\Delta\nu}{\nu} = [K(K+1) - \mathcal{K}(\mathcal{K}+1)] \times \left[\frac{\hbar}{4\pi\mu\nu} \left(\frac{1}{r_0^2} - \left\langle \frac{1}{r^2} \right\rangle_v \right) - \frac{\alpha r_0}{2\pi\hbar\nu} \frac{dV_u}{dr} \right] + \frac{\hbar}{2\pi\mu r_0^2 \nu} \,.$$

Here $\sigma^A_{v\mathcal{K}}(\nu)$ is the cross section calculated by Dunn[6] for effective rotational quantum number $\mathcal{K}$. The quantities Q_e, dQ_e/dr, and dV_u/dr are evaluated at the classical turning point in determining A and $\Delta\nu$.

Evaluation of terms shows the quantity in the large parentheses in the expression for A to be about 1×10^{-3}. The term in the large brackets in the expression for $\Delta\nu/\nu$ is about 2×10^{-4}, while the constant term is about 1×10^{-3}. We see from Eq. (A2) that a correction of this order should be applied to the calculated cross sections, and that the cross section should be shifted on the wavelength scale by a few angstroms. These corrections are ignored since they are much too small to account for the difference between experiment and predictions using a simple Franck-Condon picture.

---

*Work supported in part by the Controlled Thermonuclear Branch of the U.S. Atomic Energy Commission.

†Work done while on leave from Physikalisches Institut, University of Bonn, Bonn, Germany.

‡Staff Member, Laboratory Astrophysics Division, National Bureau of Standards.

§Of the National Bureau of Standards and the University of Colorado.

[1]D. R. Bates, Monthly Notices Roy. Astron. Soc. 112, 40 (1952).

[2]R. A. Buckingham, S. Reid, and R. Spence, Monthly Notices Roy. Astron. Soc. 112, 382 (1952).

[3]W. Linlor, C. F. Barnett, and R. G. Reinhardt, University of California Radiation Laboratory Report No. UCRL-4917, 1957 (unpublished).

[4]G. Gibson, University of California Radiation Laboratory Report No. UCRL-4671, 1956 (unpublished).

[5]G. H. Dunn, in *Atomic Collision Processes*, edited by M. R. C. McDowell (North-Holland, Amsterdam, 1964), p. 997.

[6](a) G. H. Dunn, Bull. Am Phys. Soc. 10, 181 (1965); (b) Phys. Rev. 172, 1 (1968); (c) Joint Institute for Laboratory Astrophysics Report No. 92, 1968 (unpublished).

[7]D. R. Bates, K. Ledsham, and A. L. Stewart, Phil. Trans. Roy. Soc. (London) A246, 215 (1953); D. R. Bates and R. H. G. Reid, in *Advances in Atomic and*

Molecular Physics, edited by D. R. Bates and I. Esterman (Academic, New York, 1968), Vol. 4; M. M. Madsen and J. M. Peek, At. Data 2, 171 (1971).

[8]D. R. Bates, J. Chem. Phys. 19, 1122 (1951).

[9]S. Cohen, J. R. Hiskes, and R. J. Riddell, Jr., Phys. Rev. 119, 1025 (1960).

[10]G. H. Dunn, J. Chem. Phys. 44, 2592 (1966).

[11]D. Villarejo, J. Chem. Phys. 49, 2523 (1968).

[12]S. Rothenberg and E. R. Davidson, J. Mol. Spectry. 22, 1 (1967).

[13]Yu. D. Oksjuk, Opt. i Spektroskopiya 23, 213 (1967) [Opt. Spectry. (USSR) 23, 115 (1967)].

[14]W. A. Chupka, M. E. Russell, and K. Refaey, J. Chem. Phys. 48, 1518 (1968).

[15]W. A. Chupka and J. Berkowitz, J. Chem. Phys. 48, 5726 (1968).

[16]W. A. Chupka and M. E. Russell, J. Chem. Phys. 49, 5426 (1968).

[17]W. A. Chupka and J. Berkowitz, J. Chem. Phys. 51, 4244 (1969).

[18]D. R. Bates and G. Poots, Proc. Phys. Soc. (London) A66, 784 (1953).

[19]J. Franck, Trans. Faraday Soc. 21, 536 (1925); E. U. Condon, Phys. Rev. 28, 1182 (1926).

[20]G. H. Dunn and B. Van Zyl, Phys. Rev. 154, 40 (1967).

[21]G. D. Yarnold and H. C. Bolton, J. Sci. Instr. 26, 38 (1949).

[22]Guidelines for statistical reduction of the data were followed from K. A. Brownlee, *Statistical Theory and Methodology in Science and Engineering*, 2nd ed. (Wiley, New York, 1965), Chap. 10.

[23]J. H. Moore, Jr. and J. P. Doering, J. Chem. Phys. 50, 1487 (1969).

[24]J. W. McGowan and M. A. Fineman, Phys. Rev. Letters 15, 179 (1965). These authors interpreted electron-impact threshold ionization data in terms of a considerable amount of simultaneous rotational excitation with ionization. In a later paper (Ref. 39) most of the structure originally interpreted as rotational excitation was reinterpreted in terms of autoionization.

[25]W. Kolos and L. Wolniewicz, J. Chem. Phys. 43, 2429 (1965).

[26]H. Beutler and H.-O. Jünger, Z. Physik 100, 80 (1936); 101, 285 (1936).

[27]G. R. Cook and P. A. Metzger, J. Opt. Soc. Am. 54, 968 (1964).

[28]V. H. Dibeler, R. M. Reese, and M. Krauss, J. Chem. Phys. 42, 2045 (1965).

[29]F. J. Comes and W. Lessman, Z. Naturforsch. 19a, 508 (1964).

[30]P. H. Doolittle and R. I. Schoen, Phys. Rev. Letters 14, 348 (1965).

[31]F. J. Comes and H. O. Wellern, Z. Naturforsch. 23a, 881 (1968).

[32]R. S. Berry, J. Chem. Phys. 45, 1228 (1966).

[33]S. E. Nielsen and R. S. Berry, Chem. Phys. Letters 2, 503 (1968).

[34]J. N. Bardsley, Chem. Phys. Letters 1, 229 (1967).

[35]A. Russek, M. R. Patterson, and R. L. Becker, Phys. Rev. 167, 17 (1968).

[36]J. C. Y. Chen and N. F. Lane, in *Fifth International Conference on the Physics of Electronic and Atomic Collisions: Abstracts of Papers* Nauka, Leningrad, 1967), p. 627.

[37]D. D. Briglia and D. Rapp, Phys. Rev. Letters 14, 245 (1965).

[38]P. Marmet and L. Kerwin, Can. J. Phys. 38, 972 (1960).

[39]J. W. McGowan, M. A. Fineman, E. M. Clarke, and H. P. Hanson, Phys. Rev. 167, 52 (1968).

[40]L. J. Kieffer and G. H. Dunn, Rev. Mod. Phys. 38, 1 (1966).

[41]G. M. Prok, C. F. Monnin, and H. J. Hettel, J. Quant. Spectry. Radiative Transfer 9, 361 (1969); M. Gryziński, Phys. Rev. 138, A336 (1965).

[42]M. R. Flannery and U. Öpik, Proc. Phys. Soc. (London) 86, 491 (1965).

[43]M. I. Al-Joboury and D. W. Turner, J. Chem. Soc. 5141 (1963); D. W. Turner and D. P. May, J. Chem. Phys. 45, 471 (1966); D. C. Frost, C. A. McDowell, and D. A. Vroom, Proc. Roy. Soc. (London) A296, 566 (1967); R. Spohr and E. von Puttkamer, Z. Naturforsch. 22a, 705 (1967); J. Berkowitz, H. Ehrhardt, and T. Tekaat, Z. Physik 200, 69 (1967); K. Siegbahn *et al.*, *ESCA: Atomic, Molecular, and Solid State Structure Studied by Means of Electron Spectroscopy* (Almqvist and Wiksells, Uppsala, Sweden, 1967); D. W. Turner, Proc. Roy. Soc. (London) A307, 15 (1968).

[44]D. Villarejo, J. Chem. Phys. 48, 4014 (1968).

[45]H. Hotop, in Proceedings of the International Conference on Mass Spectrometry, Brussels, 1970 (unpublished).

[46]D. F. Dance, M. F. A. Harrison, R. D. Rundel, and A. C. H. Smith, Proc. Phys. Soc. (London) 92, 577 (1967).

[47]B. Peart and K. Dolder (private communication).

[48]J. M. Peek, Phys. Rev. 154, 52 (1967).

[49]R. Caudano and J. M. Delfosse, in *Sixth International Conference on the Physics of Electronic and Atomic Collisions: Abstracts of Papers* (MIT Press, Cambridge, 1969), p. 818.

[50]J. M. Peek and T. A. Green, in *Electronic and Atomic Collisions: Abstracts of Papers of the Seventh International Conference on the Physics of Electronic and Atomic Collisions* (North-Holland, Amsterdam, 1971), p. 567.

[51]N. Bauer and J. Y. Beach, J. Chem. Phys. 15, 150 (1947).

[52]O. A. Schaeffer and J. M. Hastings, J. Chem. Phys. 18, 1048 (1950).

[53]G. H. Dunn and L. J. Kieffer, Phys. Rev. 132, 2109 (1963); L. J. Kieffer and G. H. Dunn, *ibid.* 158, 61 (1967); R. J. Van Brunt and L. J. Kieffer, Phys. Rev. A 2, 1293 (1970).

[54]A. C. Riviere and D. R. Sweetman, Phys. Rev. Letters 5, 560 (1960).

[55]See, for example: G. W. McClure, Phys. Rev. 140, A769 (1965); D. K. Gibson and J. Los, Physica 35, 258 (1967); M. Vogler and W. Seibt, Z. Physik 210, 337 (1968); R. Caudano and J. M. Delfosse, J. Phys. B 1, 813 (1968).

[56]G. H. Dunn, F. von Busch, and B. Van Zyl, in Ref. 36, p. 610.